Control of the Sawtooth Instability by Electron Cyclotron Heating and Current Drive In the TCV and ASDEX Upgrade Tokamaks.

T.P. Goodman 1), A. Mück 2), C. Angioni 1), M.A. Henderson 1), O. Sauter 1), F. Ryter 2), E. Westerhof 3), H. Zohm 2) and the ASDEX Upgrade Team 2)
1) Centre de Recherches en Physique des Plasmas, Association EURATOM - Confédération Suisse, Ecole Polytechnique Fédérale de Lausanne, CRPP - EPFL, CH-1015 Lausanne, Switzerland
2) Max-Planck-Institut für Plasmaphysik, IPP-EURATOM Ass., 85748 Garching, Germany
3) FOM-Instituur voor Plasmafysica "Rijnhuizen", Ass. EURATOM-FOM, TEC, PO Box 1207, 3430 BE Nieuwegein, NL
e-mail contact of main author: timothy.goodman@epfl.ch

Abstract: Recently, there has been increased interest in avoiding the destabilization of NTMs by controlling the sawtooth instability which frequently provides a large enough seed island to trigger the growth of the NTM. Electron cyclotron heating (ECH) and current drive (ECCD) are prime candidates for such control as the all important deposition location can be adjusted using external control parameters alone. Sawtooth control studies have been carried out on the Tokamak à Configuration Variable (TCV) and ASDEX Upgrade tokamaks. The experiments and subsequent sawtooth period modeling help to determine the optimum locations for sawtooth period control and understand the mechanism by which this control is attained.

1. Introduction

The stabilization, or at least reduction to an insignificant amplitude, of NTMs at the q=2 and q=3/2 surfaces has been demonstrated in the past [1,2,3]. It has been shown experimentally that ion-cyclotron absorption can alter the sawtooth period. By adjusting the deposition location so as to shorten the sawtooth period, the plasma beta can be increased to higher levels than in the presence of longer sawteeth, before triggering an NTM [4].

Early experiments showed that electron cyclotron resonance absorption (ECH) near the q=1 surface can drastically alter the sawtooth period [e.g. 5]. Furthermore, TCV has shown that with absorption near the q=1 surface, electron cyclotron current drive (ECCD) driving current in the same direction as the plasma current (co-ECCD) lengthens the sawtooth period over that of pure ECH. Driving current counter to the direction to the plasma current (counter-ECCD) decreases the period. Control of the deposition location can be carried out by adjusting the magnetic field strength, to move the resonance relative to the q=1 surface itself as in the case of ICRH. However, the greatest potential advantage of ECH over ICRH is that the absorption location can be easily adjusted by changing external parameters (launcher mirrors) only, thereby becoming relevant to ITER operation.

In this paper sawtooth stabilization / destabilization refers to a lengthening / shortening of the sawtooth period; although, the sawtooth crash can also be effectively eliminated by reducing the period and/or amplitude towards zero. We show the (de)stabilization of the sawtooth instability by ECH and by co- and counter- ECCD on TCV, using real-time antenna steering; and on the ASDEX Upgrade tokamak, by adjusting the magnetic field strength. The relative merits of co- and counter-ECCD are discussed and the optimum location for stabilization is shown by modeling to be outside of the q=1 surface for co-ECCD and ECH and inside this surface for strong counter-ECCD. This is consistent with the available experimental evidence. Preliminary results of a TCV experiment looking for a theoretically predicted optimum location for destabilization are also presented.

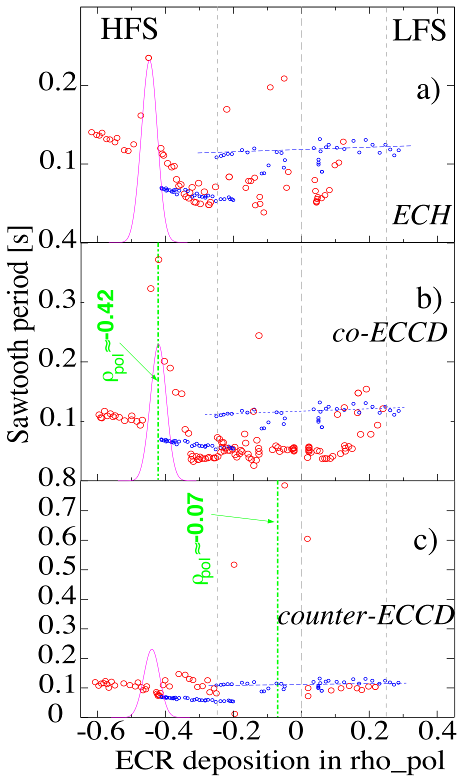

FIG. 1. Sawtooth period as a function of the deposition location for ECRH, co - and counter - CD. Vertical gray dashed lines are the HFS inversion radius, plasma center and LFS inversion radius (left to right). The locations of complete stabilization at fixed field are shown for co-CD (-0.42) and counter-CD (-0.07).

2. ASDEX Upgrade: Complete stabilization by ECCD in NBI heated plasmas [6]

In ASDEX Upgrade, stabilization has been achieved in single null, H-mode, NBI heated (ca. 5-5.3 MW), 0.8 MA plasmas using relatively low additional EC power (ca. 0.8-0.9 MW). The magnetic field is swept at a rate of ~0.1 T/s and moves the deposition location towards the LFS in time. Two gyrotrons are used with toroidal injection angles +/-15° for counter/co-ECCD, or with opposite signs for ECH. This ensures equivalent absorption locations and widths for the three cases. The results are summarized in Figures 1a-c, each showing combinations of shots with toroidal field sweeps for ECH, co- and counter- ECCD. The sawtooth period (red) is plotted versus the deposition location of the EC power in normalized radius (calculated by the TORBEAM code); $\rho_{pol} < 0$ indicates high field side (HFS) deposition. The sawtooth periods from NBI-only heated shots are shown in small points (blue), for reference. The step in the sawtooth period near the inversion radius is due to a change in the NBI sources [6]. A sample deposition profile is shown on each plot; scaled with the sawtooth period axis. It is chosen to match the sawtooth period peak height for ECH. It has been shown on TCV that when the sawtooth period is linear in ECH power density, the width of the peak in sawtooth period can be used as an approximate measure of the beam width [7, 8].

Heating and especially co-ECCD are stabilizing when absorbed near ρ_{pol} = -0.42; well outside of the sawtooth inversion radius of ρ_{pol} = - 0.25. This peak in period is consistent with changing the growth rate of the shear at the q=1 surface (see below). The addition of co-ECCD further inside this peak, but still outside the inversion radius, ($|\rho_{pol}|$~0.25 - 0.35) decreases the sawtooth period relative to that measured with ECH (i.e. co-ECCD is destabilizing) while counter-ECCD increases the period. With counter-ECCD heating near ρ_{pol} = -0.42 produces sawtooth periods shorter than those found using ECH in accord with results on TCV. There is a broad stabilization region with near-central deposition, as shown in Figure 1c, consistent with a flattening of the central q-profile. The q=1 surface should still exist, however, as a m=1, n=1 mode is present. Complete stabilization was achieved with deposition at ρ_{pol} = -0.07. No direct measure of the current profile (MSE) was available for these shots.

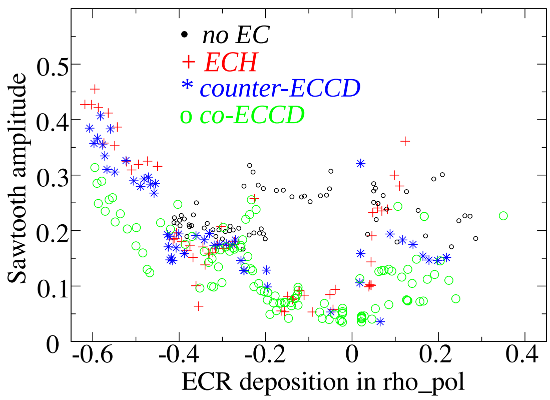

FIG. 2. Sawtooth amplitude as a function of deposition radius for the same swept magnetic field shots presented in Figure 1.

In Figure 2, the sawtooth amplitudes from the shots of Figure 1 are shown. For $\rho_{pol} < -0.42$, both the period and amplitude decrease in the order: ECH, counter-ECCD and co-ECCD. In other regions there are various sawtooth shapes similar to [9]. Note that there is a clear asymmetry between LFS and HFS deposition in both the sawtooth period and amplitude. This may be due to the generation of a larger trapped electron fraction when heating on the LFS.

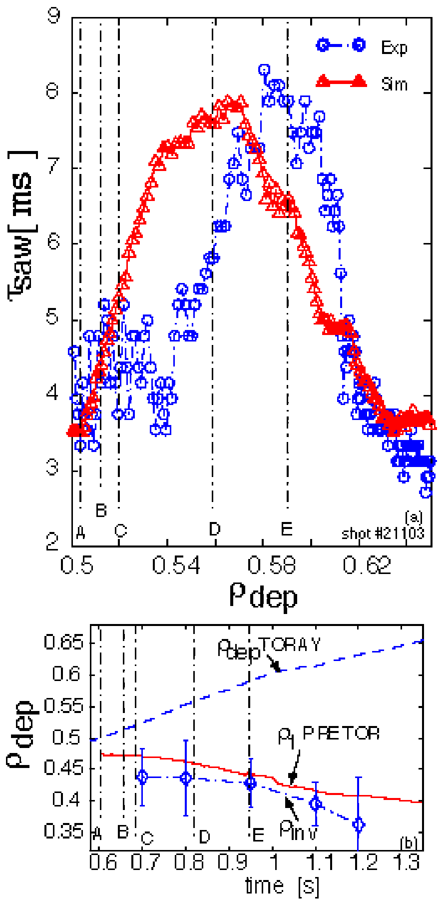

FIG. 3. Sawtooth simulations during swept ECH deposition accurately reproduces the TCV experimental sawtooth period (a) and the q-profile evolution (b). The horizontal scale of figure (a) corresponds to 15% of the plasma radius. The maximum in the sawtooth period (D/E) is found with the deposition well outside the inversion radius and the q=1 surface.

3. TCV: Optimum absorption location for sawtooth stabilization

In sweep experiments which use only external control parameters (i.e. no magnetic field sweep) and which cover the largest possible range of ρ_{dep}, it is difficult to combine several independent beams at precisely the same ρ_{dep}; especially when aiming from above and below the plasma midplane. The resonance should pass through the plasma center and thus the transverse dimension of the beam is nearly perpendicular to the flux surfaces as $\theta_{pol} \sim \pm 90°$. If the resonance is roughly tangent to the flux surface at the deposition location, (i.e $\theta_{pol} \sim 0°$ or $180°$) ρ_{dep} is relatively insensitive to aiming angles and beam width.

While plasmas swept vertically through an ECH beam have been used to improve the accuracy of the LIUQE equilibrium reconstruction code [10] and therefore the ability to overlap multiple beams; some systematic discrepancies between magnetic and tomographic measurements [11] remain to be elucidated and absolute measurements below ± 5% of minor radius are not possible. Nevertheless, sweeps still provide precise, reproducible, *relative* measurements. The sensitivity of the sawtooth period to power density is used to align launchers, in situ, to within ~±10% of the beam width (i.e. ±1% minor radius) at TCV [7]. Fortunately, sawtooth period modelling can provide testable predictions based on relative measurements.

Sawtooth experiments are analyzed using the PRETOR-ST [8 and Ref.s therein] transport code, linked to a sawtooth period model first proposed to predict the sawtooth period in an ITER burning plasma. Many stabilizing terms can be taken into account, and in this form, the model has been successful in correctly simulating the sawtooth period variation during *a)* experiments with swept ECH beams in TCV [12], *b)* NBI heated plasmas in JET [13] – with fast-particle stabilization of sawteeth – and *c)* ICRH/ICCD heated JET discharges with negligible fast-particle stabilization [8]. Moreover, the code can separate the influence of current drive from that of the accompanying heating [8]. In actual experiments, both are always present simultaneously.

Figure 3 shows that the calculated deposition location for optimum sawtooth stabilization is in good agreement with the experimental results using ~1.3MW of swept ECH in a plasma of I_p ~ 350kA, κ ~ 1.7, δ ~ 0.45 and n_{e0} ~ $3•10^{19}m^{-3}$. The optimum is clearly outside the experimentally measured inversion radius (from x-ray tomography) and the q=1 surface (calculated self-consistently by PRETOR-ST). As the EC absorption moves outside of the q=1 surface, the q=1 radius decreases as also seen with the LIUQE equilibrium reconstruction code.

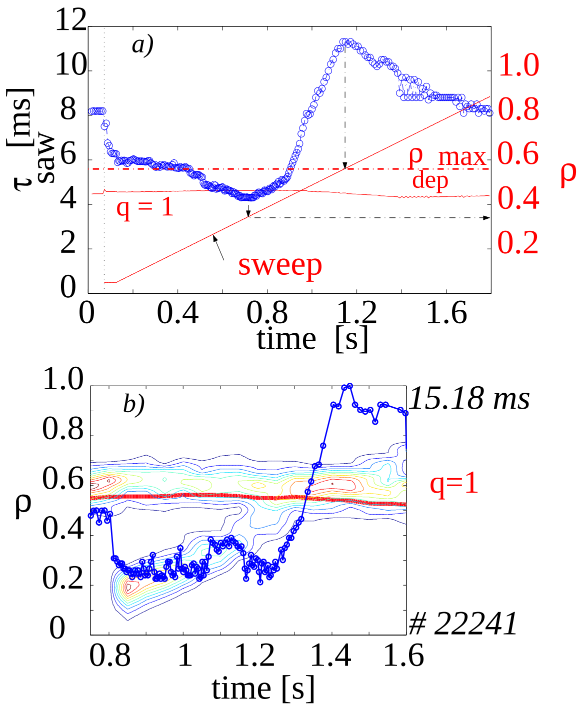

FIG. 4. a) Simulation: 1.3MW ECH fixed for optimum stabilization; 0.45MW of swept ECH. Sawtooth period, q=1 and ρ_{dep} are shown. b) Experimental sawtooth period, LIUQE q=1 (red line) and TORAY ECH power density contours: 0.9MW ECH (slight co-ECCD) fixed for optimum stabilization; 0.45MW of swept ECH (slight co-ECCD). ECH destabilizes sawteeth, inside q=1.

It is expected that the sawtooth model will show similar accord between ρ_{dep} and the sawtooth period for the ASDEX Upgrade results presented above. However, since the various NBI sources produce different sawtooth periods on ASDEX Upgrade, the model must now simultaneously simulate the effects of NBI stabilization, as well as the evolution of the shear at q=1 (s_1) and critical shear (s_{1crit}) due to ECH/ECCD: the crash condition for the later case being simply $s_1 > s_{1crit}$. While fast-particle stabilization may play a role during NBI heating, the different NBI sources have different deposition profiles and may also affect the sawteeth in the same way as the ECH. In addition, changes in the rotation profile can also affect the sawtooth period [14].

4. Predicted Optimum Location for Sawtooth Destabilization.

The stabilizing effect of Figure 3 can be eliminated by the addition of ~0.5MW of ECH absorbed at a fixed location ρ_{dep} ~ 75%$\rho_{inversion}$ [8]; thus, ECH might be able to destabilize the long period sawteeth predicted in burning plasmas. PRETOR-ST predicts that the sawtooth period will exhibit a minimum (destabilization) at a distance inside the q=1 surface roughly equal to the Gaussian half-width of the ECH beam [8]. In the simulation, 1.35 MW are deposited at the optimum location for stabilization outside of q=1 while a fourth beam is swept from inside to outside the q=1 surface. The sawtooth period is calculated as a function of the deposition radius of the swept beam (Fig. 4a).

In a preliminary experiment to test this prediction, 0.9MW of power was used at fixed injection angle to simplify the overlap of the stabilizing beams. In addition, a small co-ECCD component due to the poloidal field is also present. This should cause the maximum found in the simulation (heating only) to shift slightly inward and the minimum slightly outward [8]. The additional co-ECCD will also increase the sawtooth period at the maximum relative to pure heating as shown on ASDEX Upgrade (Fig. 1). On TCV an additional beam was swept, similar to the simulation. The results are presented in Fig. 4b as a function of time and ρ. The EC power density contours are shown along with the LIUQE q=1 radius (thick red line). The sawtooth period (normalized to the maximum) is then overlaid as a function of time. Starting from the stabilized sawtooth period (t< 0.8s), *a)* the central beam is destabilizing (t>0.8s), *b*) a small minor peak is found (t~1.1s) and finally, *c*) the beam crosses the location of the other 2 beams (t>1.4s) with a further increase in the sawtooth period. Following the minor peak, a minimum is seen in the period (t~1.2s) but, the period is not shorter than that found at the start of the sweep (the sawtooth amplitude, however, exhibits a minimum only at t~1.2s).

When the central beam is added, a strong m=1, n=1 mode is present as in saturated sawteeth [9,15]. At the minor peak some similarities are seen with sawteeth interpreted as exhibiting partial magnetic reconnection [15] for which a more complete, 2D model of the sawtooth crash [16] is needed. Unfortunately, the 2D model used to match the sawtooth shape, cannot predict the sawtooth period.

5. Conclusions

Both TCV and ASDEX Upgrade show stabilization of the sawtooth period with power deposition outside of the inversion radius (and q=1 for TCV) as in the sawtooth model. The sawtooth model may be in accord with ASDEX Upgrade results showing sawtooth destabilization inside inversion radius with co-ECCD and stabilization with counter-ECCD. Modeling of ASDEX Upgrade results is still to be carried out and is complicated by simultaneous NBI heating effects. Preliminary TCV experiments to find the predicted optimum destabilization location inside q=1 show destabilization over a broad range of deposition locations and 2D sawtooth features which are out of the range of application of the sawtooth model used in PRETOR-ST.
This work was partly supported by the Swiss National Science Foundation.

6. References

[1] ZOHM, H., et al., Nuclear Fusion 39 (1999) 577.
[2] LA HAYE, R.J., et al., Phys. of Plasmas 9 (2002) 2051.
[3] ISAYAMA, A., et al., Plasma Phys. Control. Fusion 42 (2000) L37.
[4] SAUTER, O., et al., Phys. Rev. Lett. 88 (2002) 105001.
[5] HANADA, K., et al., Phys. Rev. Lett. 66 (1991) 1974.
[6] MÜCK, A., et al., in Proc. of 29th EPS Conf. on Plasma Phys. and Control. Fusion., Montreux, 2002 [ECA 26B (2002) P1.037].
[7] HENDERSON, M.A., et al., Fusion Engineering and Design, 53 (2001) 241.
[8] ANGIONI, C., et al., Submitted to Nuclear Fusion; ANGIONI, C., et al., in Proc. of 29th EPS Conf. on Plasma Phys. and Control. Fusion., Montreux, 2002 [ECA 26B (2002) P1.118].
[9] PIETRZYK, Z.A., et al., Nucl. Fusion 39 (1999) 587.
[10] GOODMAN, T.P., TCV Team, Proc. of IAEA-FEC, Sorento, 2000, [IAEA, Vienna (2001) EXP4/09].
[11] MLYNAR, J., et al., Lausanne Internal report LRP 732/02.
[12] ANGIONI, C., et al., in Theory of Fusion Plasmas, (Proc. Joint Varenna-Lausanne Int. Workshop) (Varenna 2000), edited by J.W. Connor, O. Sauter and E. Sindoni, ISPP-19 (Bologna, Editrice Compositori) (2000) 73.
[13] ANGIONI, C., et al., Plasma Phys. Control. Fusion 44, (2002) 205.
[14] GRAVES, J., et al., to be published in Theory of Fusion Plasmas (Proc. Joint Varenna-Lausanne Int. Workshop) (Varenna 2002), edited by J.W. Connor, O. Sauter and E. Sindoni, ISPP-20 (Bologna, Editrice Compositori) (2002).
[15] FURNO, I., et al., Nucl. Fusion 41 (2001) 403.
[16] PORCELLI, F., et al., Phys. Rev. Lett. 82 (1999) 1458.